Syntheses, Structures, and Properties of Tetrakis(*μ*-acetato)dirhodium(II) Complexes with Axial Pyridine Nitrogen Donor Ligands with or without Assistance of Hydrogen Bonds

Hideki Kitamura,[†] Tomohiro Ozawa,[‡] Koichiro Jitsukawa,*[,†] Hideki Masuda,*[,†,||] Yasuhiro Aoyama,[§,⊥] and Hisahiko Einaga[†]

Department of Applied Chemistry, Nagoya Institute of Technology, Showa-ku, Nagoya 466-8555, Japan, Coordination Chemistry Laboratories, Institute for Molecular Science, Okazaki 444-8585, Japan, The Institute for Fundamental Research of Organic Chemistry, Kyushu University, Hakozaki, Higashi-ku, Fukuoka 812-8581, Japan, and CREST, Japan Science and Technology Corporation (JST), Hakozaki, Higashi-ku, Fukuoka 812-8581, Japan

Received October 12, 1999

Eight adducts of $Rh_2(O_2CCH_3)_4$ with axial pyridine derivatives that contain hydrogen-bonding amino and/or steric methyl substituents in the 2- and 6-positions have been prepared and examined by electronic absorption and ^1H NMR spectroscopy in solution and by elemental, IR, thermogravimetric, and X-ray diffraction analyses in the solid state. The results indicated that strong hydrogen bonding interactions between $Rh_2(O_2CCH_3)_4$ and axially coordinated pyridine derivatives with a 2- or 6-amino group occur in both solution and the solid state and contribute to the higher thermal stability of the molecular assembly of dirhodium complexes. It was demonstrated that such a combination of coordinate and hydrogen bonds is useful as a building tool in designing and constructing new organic−inorganic hybridized compounds and supramolecular architectures.

Introduction

Recently we reported a unique complex of $[Rh_2(O_2CCH_3)_4]$−$[Ni(biphenylbiguanidado)_2]$ as a new organic−inorganic hybridized compound,[1] which formed an infinite one-dimensional chain structure assembled with coordinate and hydrogen bonds. Such a novel approach for the construction of hybridized compounds allows us to anticipate unique electronic properties, for example, nonlinear optical behavior, electric conductivity, and magnetism.[2−5] The design and syntheses of molecular assemblies using coordinate bonds are currently of intense interest in chemistry.[6−9] Besides covalent bonds, control of the hydrogen bond, which is also an efficient organizing force in the design of solid-state materials,[10−12] is a strategy for achieving the formation of supramolecular architectures because of its directionality and appropriate strength. Previously, we[13] and others[14] have reported some hydrogen-bond-assembled supramolecular structures. Introduction of hydrogen bonds into metal complexes, as described previously for complex $[Rh_2(O_2CCH_3)_4]$-$[Ni(biphenylbiguanidado)_2]$,[1] may provide new materials with

* To whom correspondence should be addressed.
[†] Nagoya Institute of Technology.
[‡] Institute for Molecular Science.
[§] Kyushu University.
[||] Phone: (052)735-5228. Fax: (052)735-5247. E-mail: masuda@ach.nitech.ac.jp.
[⊥] Japan Science and Technology Corporation (JST).

(1) Kitamura, H.; Ozawa, T.; Jitsukawa, K.; Masuda, H.; Einaga, H. *Chem. Lett*. **1999**, 1225.
(2) (a) Barrows, A. D.; Chang, C. W.; Chowdhry, M. M.; McDrady, J. E.; Mingos, D. M. P. *Chem. Soc. Rev*. **1996**, *25*, 329. (b) Barrows, A. D.; Mingos, D. M. P.; White, A. J. P.; Williams, D. J. *J. Chem. Soc., Chem. Commun*. **1996**, 97. (c) Barrows, A. D.; Mingos, D. M. P.; White, A. J. P.; Williams, D. J. *J. Chem. Soc., Dalton Trans*. **1996**, 149.
(3) Tadokoro, M.; Isobe, K.; Uekusa, H.; Ohashi, Y.; Toyoda, J.; Tashiro, K.; Nakasuji, K. *Angew. Chem., Int. Ed. Engl*. **1999**, *38*, 95.
(4) Lawrence, D. S.; Jiang, T.; Levett, M. *Chem. Rev*. **1995**, *95*, 2229.
(5) (a) Ward, M. D. *Chem. Soc. Rev*. **1997**, *26*, 365. (b) de Rege, P. J. F.; Williams, S. A.; Therien, M. J. *Science* **1995**, *269*, 1409. (c) Tecilla, P.; Dixon, R. P.; Slobodkin, G.; Alavi, D. S.; Waldeck, D. H.; Hamilton, A. D. *J. Am. Chem. Soc*. **1990**, *112*, 9408. (d) Sessler, J. L.; Wang, B.; Harriman, A. *J. Am. Chem. Soc*. **1995**, *117*, 704. (e) Bernhardt, P. V.; Hayes, E. J. *Inorg. Chem*. **1998**, *37*, 4214. (f) White, C. M.; Gonzalez, M. F.; Bardwell, D. A.; Rees, L. H.; Jeffery, J. C.; Ward, M. D.; Armaroli, N.; Calogero, G.; Barigelletti, F. *J. Chem. Soc., Dalton Trans*. **1997**, 727.
(6) (a) Stang, P. J.; Olenyuk, B. *Acc. Chem. Res*. **1997**, *30*, 502. (b) Linton, B.; Hamilton, D. *Chem. Rev*. **1997**, *97*, 1669. (c) Fyee, M. C. T.; Stoddart, J. F. *Acc. Chem. Res*. **1997**, *30*, 393. (d) Jones, C. J. *Chem. Soc. Rev*. **1998**, *27*, 289.
(7) (a) Lu, J.; Paliwala, T.; Lim, S. C.; Yu, C.; Niu, T.; Jacobson, A. J. *Inorg. Chem*. **1997**, *36*, 923. (b) Duncan, P. C. M.; Goodgame, D. M. L.; Menzer, S.; Williams, D. J. *J. Chem. Soc., Chem. Commun*. **1996**, 2127.
(8) (a) Lehn, J.-M. *Pure Appl. Chem*. **1971**, *50*, 871. (b) Lehn, J.-M. *Supramolecular Chemistry*; VCH: Basel, 1995.
(9) (a) Fujita, M.; Ogura, D.; Miyazawa, M.; Oka, H.; Yamaguchi, K.; Ogura, K. *Nature* **1995**, *378*, 469. (b) Takeda, N.; Umemoto, K.; Yamaguchi, K.; Fujita, M. *Nature* **1999**, *398*, 794.
(10) (a) Zerkowski, J. A.; MacDonald, J. C.; Whitesides, G. M. *Chem. Mater*. **1997**, *9*, 1933. (b) Simanek, E. E.; Tsoi, A.; Wang, C. C. C.; Whitesides, G. M. *Chem. Mater*. **1997**, *9*, 1954. (c) MacDonald, J. C.; Whitesides, G. M. *Chem. Rev*. **1994**, *94*, 2383. (d) Bernstein, J.; Davis, R. E.; Shimoni, L.; Chang, N.-L. *Angew. Chem., Int. Ed. Eng*. **1995**, *34*, 1555.
(11) Branda, N.; Wyler, R.; Rebek, J., Jr. *Science* **1994**, *263*, 1267.
(12) (a) Endo, K.; Sawaki, T.; Koyanagi, M.; Masuda, H.; Aoyama, Y. *J. Am. Chem. Soc*. **1995**, *117*, 8341. (b) Endo, K.; Ezuhara, T.; Koyanagi, M.; Masuda, H. Aoyama, Y. *J. Am. Chem. Soc*. **1997**, *119*, 499. (c) Endo, K.; Koike, T.; Sawaki, T.; Hayashida, O.; Masuda, H.; Aoyama, Y. *J. Am. Chem. Soc*. **1997**, *119*, 4117.
(13) (a) Kitamura, H.; Ozawa, T.; Jitsukawa, K.; Masuda, H.; Einaga, H. *Mol. Cryst. Liq. Cryst*. **1996**, *285*, 281. (b) Ohata, N.; Masuda, H.; Yamauchi, O. *Angew. Chem., Int. Ed. Eng*. **1996**, *35*, 531. (c) Mizutani, M.; Jitsukawa, K.; Masuda, H.; Einaga, H. *Inorg. Chim. Acta* **1998**, *283*, 105.
(14) (a) Kawata, S.; Kitagawa, S.; Kondo, M.; Furuti, I.; Munakata, M. *Angew. Chem., Int. Ed. Eng*. **1994**, *33*, 1759. (b) Batsnov, A. S.; Begkey, M. J.; Hubberstey, P.; Stroud, J. *J. Chem. Soc., Dalton Trans*. **1995**, 1947. (c) Munakata, M.; Wu, L. P.; Yamamoto, M.; Kuroda-Sowa, T.; Maekawa, M. *J. Am. Chem. Soc*. **1996**, *118*, 3117.

10.1021/ic991200i CCC: $19.00
Published on Web 06/24/2000

Chart 1

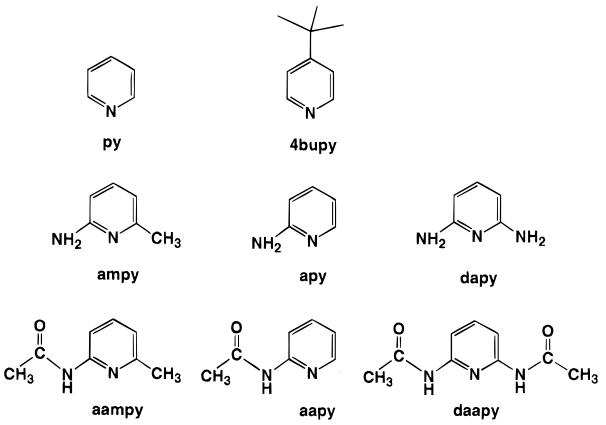

interesting properties by simultaneous contributions of hydrogen and coordinate bonds.

To examine the effect of hydrogen bonds in the molecular assembly of $[Rh_2(O_2CCH_3)_4X_n]$ associated with coordinate and hydrogen bonds, eight adducts of $Rh_2(O_2CCH_3)_4$ with various axial pyridine derivatives (X = pyridine (py), 4-*tert*-butylpyridine (4bupy), 2-amino 6-methylpyridine (ampy), 2-aminopyridine (apy), 2,6-diaminopyridine (dapy), 2-acetylamino-6-methylpyridine (aampy), 2-acetylamino pyridine (aapy), and 2,6-diacetylaminopyridine (daapy) (Chart 1)) have been prepared. The structures and properties were investigated by electronic absorption and ^{1}H NMR spectroscopies in solution and by elemental, X-ray, and thermogravimetric analyses and IR spectroscopy in the solid state.

Experimental Section

Materials. Some chemical reagents employed here as axial ligands, pyridine (py), 2-aminopyridine (apy), 2,6-diaminopyridine (dapy), 2-amino-6-methylpyridine (ampy), 4-*tert*-butylpyridine (4bupy), and pivalic acid, were purchased from Tokyo Chemical Industry and were of analytical grade or the highest grade available. The acetyl derivatives of apy, ampy, and dapy (2-acetylaminopyridine (aapy), 2-acetylamino-6-methylpyridine (aampy), and 2,6-acetylaminopyridine (daapy), respectively) were prepared according to the usual method. $Rh_2(O_2CCH_3)_4$ (**1**) was prepared according to the literature.[15]

Preparations. a. $[Rh_2(O_2CCH_3)_4(py)_2]$ (2). Complex **2** was prepared according to the literature.[16]

b. $[Rh_2(O_2CCH_3)_4(4bupy)_2]$ (3). To an acetone solution of **1** was added a large excess of 4bupy to directly prepare the sample as red precipitate (yield: 86% based on **1**). ^{1}H NMR ($CDCl_3$): δ 1.45 (s, 18H, *t*-Bu), 1.91 (s, 12H, $-CH_3$), 7.67 (d, 4H, J = 5.1 Hz, 3-H), 9.26 (d, 4H, J = 4.8 Hz, 2-H). Anal. Calcd for $C_{26}H_{38}N_2O_8Rh_2$: C, 43.84; H, 5.38; N, 3.92. Found: C, 43.58; H, 5.36; N, 3.83.

c. $[Rh_2(O_2CCH_3)_4(ampy)_2]$ (4). To an acetone solution of **1** was added a large excess of ampy to directly prepare the sample in a crystalline form (deep-purple) that was suitable for X-ray crystal structure analysis (yield: 63% based on **1**). ^{1}H NMR ($CDCl_3$): δ 1.95 (s, 12H, CH_3COO^-), 2.60 (s, 12H, 6-CH_3), 5.10 (s, 4H, NH), 6.48 (d, 2H, J = 8.4 Hz, 3-H), 6.63 (d, 2H, J = 7.5 Hz, 5-H), 7.42 (t, 2H, J = 4.8 Hz, 4-H). Anal. Calcd for $C_{20}H_{28}N_4O_8Rh_2$: C, 34.31; H, 3.84; N, 8.89. Found: C, 34.16; H, 3.74; N, 8.71.

d. $[Rh_2(O_2CCH_3)_4(apy)_2]$ (5). To an acetone solution containing **1** was added a large excess of apy to directly prepare the sample as a reddish-purple precipitate (yield: 79% based on **1**). ^{1}H NMR ($CDCl_3$): δ 1.92 (s, 12H, CH_3COO^-), 5.49 (s, 4H, NH_2), 6.76 (d, 2H, J = 8.4 Hz, 3-H), 6.89 (t, 2H, J = 6.0 Hz, 4-H), 7.64 (t, 2H, J = 7.8 Hz, 4-H), 8.53 (d, J = 4.5 Hz, 6-H). Anal. Calcd for $C_{18}H_{24}N_4O_8Rh_2$: C, 36.49; H, 4.29; N, 8.51. Found: C, 38.46; H, 4.23; N, 8.42.

e. $[Rh_2(O_2CCH_3)_4(dapy)]$ (6). To an aqueous solution containing **1** was added a large excess of dapy to directly prepare the sample in a crystalline form (deep-purple) that was suitable for X-ray crystal structure analysis (yield: 54% based on **1**). ^{1}H NMR (acetone-d_6): δ 1.78 (s, 12H, CH_3COO^-), 5.22 (s, 8H, NH), 5.85 (d, 4H, J = 7.8 Hz, 3-H), 7.15 (t, 2H, J = 7.18 Hz, 4-H). Anal. Calcd for $C_{13}H_{19}N_3O_8Rh_2$: C, 28.33; H, 3.48; N, 7.63. Found: C, 28.53; H, 3.36; N, 7.60.

f. $[Rh_2(O_2CCH_3)_4(aampy)_2]$ (7). To an acetone solution containing **1** was added a large excess of aampy to directly prepare the sample in a crystalline form (blue) that was suitable for X-ray crystal structure analysis (yield: 81% based on **1**). ^{1}H NMR ($CDCl_3$): δ 1.99 (s, 12H, CH_3COO^-), 2.00 (s, 6H, 6-CH_3), 2.77 (s, 6H, CH_3CO-), 7.11 (d, 2H, J = 7.8 Hz, 3-H), 7.78 (t, 2H, J = 7.8 Hz, 4-H), 8.23 (d, 2H, J = 7.8 Hz, 5-H), 9.23 (s, 2H, NH). Anal. Calcd for $C_{24}H_{32}N_4O_{10}Rh_2$: C, 38.83; H, 4.35; N, 7.55. Found: C, 38.75; H, 4.36; N, 7.48.

g. $[Rh_2(O_2CCH_3)_4(aapy)_2]$ (8). To an acetone solution containing **1** was added a large excess of aapy to directly prepare the sample as purple precipitate (yield: 82% based on **1**). ^{1}H NMR ($CDCl_3$): δ 1.96 (s, 12H, CH_3COO^-), 2.09 (s, 6H, CH_3CO-), 7.35 (t, 2H, J = 7.5 Hz, 5-H), 8.00 (t, 2H, J = 8.1 Hz, 4-H), 8.59 (d, 2H, J = 7.5 Hz, 3-H), 8.78 (d, 2H, J = 7.5 Hz, 6-H), 9.66 (s, 2H, NH). Anal. Calcd for $C_{22}H_{28}N_4O_{10}Rh_2$: C, 36.99; H, 3.95; N, 7.84. Found: C, 37.17; H, 4.04 N, 7.94.

h. $[Rh_2(O_2CCH_3)_4(daapy)_2]$ (9). To an acetone solution containing **1** was added a large excess of daapy to directly prepare the sample in a crystalline form (blue) that was suitable for X-ray crystal structure analysis (yield: 74% based on **1**). ^{1}H NMR ($CDCl_3$): δ 1.96 (s, 12H, CH_3COO^-), 2.03 (s, 12H, CH_3CO-), 8.01 (t, 2H, J = 8.1 Hz, 4-H), 8.21 (d, 4H, J = 7.8, Hz, 3-H), 9.20 (s, 4H, NH). Anal. Calcd for $C_{26}H_{34}N_6O_{12}Rh_2$: C, 37.70; H, 4.14; N, 10.14. Found: C, 37.58; H, 4.03; N, 10.02.

i. $[Rh_2(pivalato)_4]$ (10). Complex **10** was prepared according to the modified method of the literature.[9] ^{1}H NMR ($CDCl_3$): δ 1.01 (s, 36H, $-CH_3$). Anal. Calcd for $C_{26}H_{34}N_6O_{12}Rh_2$: C, 37.70; H, 4.14; N, 10.14. Found: C, 37.58; H, 4.03; N, 10.02.

Spectral Measurements. Electronic absorption spectra were recorded on a JASCO Ubest-35 spectrophotometer, in quartz cells with an optical path length of 1.0 cm for a 1 mM solution at room temperature. ^{1}H NMR spectra were obtained on a Varian Gemini XL-300 spectrometer in acetone-d_6 or $CDCl_3$ with TMS as an internal standard. Samples for all measurements were freshly prepared before use. Solid-state IR spectra were measured on a JASCO FT/IR-410 spectrometer.

Thermogravimetric Analysis (TG). TG measurements were performed in static air with a Rigaku TAS 300 system equipped with a TG 8101 D. The heating rate was 5 K min^{-1}, and Al_2O_3 was used as a reference material. Samples were packed loosely in Al crucibles. The total weight loss from room temperature to 250 °C was calculated as a percentage from TG curves.

X-ray Crystal Structure Analyses of Complexes 4, 6, 7, and 9. Single-crystal X-ray diffraction data for crystals **4**, **6**, **7**, and **9** were collected at 295 K on a Rigaku RAXIS-IV imaging plate area detector with graphite monochromated Mo Kα radiation (λ = 0.710 73 Å) and a rotating anode generator. Indexing was performed from three oscillation images that were exposed for 5.0 min. The detector swing angle was 2.00°. The crystal-to-detector distance was 120.00 mm with the detector at the zero swing position. Readout was performed in the 0.100 mm pixel mode. The precise unit cell parameters were measured at 295 K by using a Rigaku AFC-7R four-circle automated diffractometer with graphite monochromated Mo Kα radiation. The crystal data and details of the parameters associated with data collection for crystals **4**, **6**, **7**, and **9** are given in Table 1. The reflection data were corrected for Lorentz and polarization effects.

The structures of all the complexes were solved by a combination of direct method and Fourier techniques and refined anisotropically for non-hydrogen atoms by full-matrix least-squares calculations. Refinements were continued until all shifts were smaller than one-third of the standard deviations of the parameters involved. Atomic scattering factors and anomalous dispersion terms were taken from the

(15) Winkhaus, G.; Ziegler, P. *Z. Anorg. Allg. Chem.* **1967**, *350*, 51.
(16) Koh, Y. B.; Christoph, G. G. *Inorg. Chem.* **1978**, *17*, 2590.

Table 1. Crystal Data and Experimental Details for Crystals 4, 6, 7, and 9

	4	**6**	**7**	**9**
formula	$C_{20}H_{28}N_4O_8Rh_2$	$C_{13}H_{19}N_3O_8Rh_2$	$C_{12}H_{16}N_2O_5Rh$	$C_{13}H_{17}N_3O_6Rh_2$
fw	658.28	551.12	371.17	414.20
cryst size/mm	0.20 × 0.20 × 0.20	0.20 × 0.20 × 0.15	0.20 × 0.15 × 0.15	0.20 × 0.20 × 0.10
cryst system	triclinic	monoclinic	monoclinic	monoclinic
space group	$P\bar{1}$	$P2_1/a$	$P2_1/n$	$P2_1/c$
a/Å	11.207(8)	8.216(3)	9.310(2)	9.873(2)
b/Å	13.573(5)	15.539(2)	10.682(4)	10.999(7)
c/Å	8.09(1)	14.229(2)	15.181(4)	15.100(6)
α/deg	94.7(1)			
β/deg	93.17(10)	94.89(3)	104.95(2)	104.83(2)
γ/deg	96.39(6)			
V/Å^3	1215(2)	1810.1(6)	1458.7(6)	1585(1)
Z	2	4	4	4
D_{calc}/g cm^{-3}	1.815	2.022	1.690	1.735
F(000)	648.0	1088.0	748.0	836.0
μ(Mo Kα)	14.08	18.66	11.87	11.09
$2\theta_{max}$/deg	55.0	51.4	51.6	51.4
no. refls measd	5869	3159	2754	2621
no. refls obsd ($I > 3\sigma(I)$)	3730	2620	2373	2006
no. variables	418	310	244	275
GOF	1.58	1.04	1.22	1.01
R	0.100	0.080	0.057	0.050
R_w	0.165	0.112	0.075	0.078
largest residuals/e Å^{-3}	0.78, −0.36	1.02, −0.94	1.03, −1.30	1.12, −0.82

literature.[18] All the hydrogen atoms were located from the difference Fourier maps, and their parameters were isotropically refined. The R and R_w values were 0.100 and 0.165 for **4**, 0.079 and 0.110 for **6**, 0.057 and 0.075 for **7**, and 0.050 and 0.078 for **9**. The weighting scheme $w^{-1} = \sigma^2(F_o)$ was employed for all the crystals. The final difference Fourier maps did not show any significant features for all the crystals. The calculations were performed on an IRIS Indigo XS-24 computer using the program teXsan.[19]

Results and Discussion

Preparation. Reaction of $Rh_2(O_2CCH_3)_4$ (**1**) with excess amounts of the axial pyridine derivatives, X, in an acetone or aqueous solution gave the complex $[Rh_2(O_2CCH_3)_4X_n]$ ($n = 1$ or 2) as a precipitate. The composition of the various complexes was determined by elemental analysis as follows: $[Rh_2(O_2CCH_3)_4(py)_2]$ (**2**), $[Rh_2(O_2CCH_3)_4(4bupy)_2]$ (**3**), $[Rh_2(O_2CCH_3)_4(ampy)_2]$ (**4**), $[Rh_2(O_2CCH_3)_4(apy)_2]$ (**5**), $[Rh_2(O_2CCH_3)_4(dapy)]$ (**6**), $[Rh_2(O_2CCH_3)_4(aampy)_2]$ (**7**), $[Rh_2(O_2CCH_3)_4(aapy)_2]$ (**8**), and $[Rh_2(O_2CCH_3)_4(daapy)_2]$ (**9**). Complex **2** was completely insoluble in water and in several organic solvents. All the remaining complexes exhibited a slight solubility in acetone and/or $CHCl_3$ except complex **6**, which dissolved only in acetone. Standing of solutions of **4**, **6**, **7**, and **9** for a few days yielded single crystals suitable for X-ray structure determination.

Electronic Absorption Spectra. Electronic absorption spectral data of $Rh_2(O_2CCH_3)_4X$ systems in acetone and/or $CHCl_3$ are summarized in Table 2. These complexes show characteristic absorption bands in the visible region that are assignable to a π^*(RhRh) → σ^*(RhRh) transition.[20b,c,21] In general, the transition shows a larger blue shift when the complex is coordinated to a stronger axial ligand[21] compared with the absorption peak of $Rh_2(O_2CCH_3)_4$ without any axial ligands. Complex **10** exhibited an intense peak at 622 nm in $CHCl_3$. The absorption spectra of complexes **3**−**5** and **7**−**9**, shown in Table 2, exhibited almost identical values in acetone and $CHCl_3$, indicating that the axial ligands of the complexes are not replaced by an acetone molecule. If the value for **10** is assigned as the absorption peak of the dirhodium complex without an axial ligand, the coordination strength of the pyridine derivatives toward $Rh_2(O_2CCH_3)_4$ is deduced as follows: 4bupy (pyridine derivative without any substituent groups in the 2- and 6-positions) > aapy, apy (those with a 2-amino group) > dapy, daapy (those with 2,6-diamino groups) > ampy, aampy (those with 2-amino and 6-methyl groups). The above findings suggest that coordination of the pyridine derivatives, with amino and/or methyl groups, to the dirhodium complex is weakened because of steric repulsion of amino and/or methyl groups with acetato groups. Interestingly, the absorption spectrum of the complex with two amino groups shows a slightly larger blue shift in comparison with those with both amino and methyl groups and indicates a significant contribution from the hydrogen bond to strong coordination with the Rh atoms.

Table 2. Electronic Absorption Spectral Data for $Rh_2(O_2CMe)_4$−X Systems in the Visible Region

X	λ_{max}/nm (ϵ/M^{-1} cm^{-1}) in $CHCl_3$	λ_{max}/nm (ϵ/M^{-1} cm^{-1}) in acetone
py	*a*	*a*
4bupy	519 (270)	517 (260)
ampy	593 (230)	596 (270)
apy	532 (260)	535 (240)
dapy	*a*	573 (280)
aampy	592 (200)	601 (260)
aapy	531 (250)	543 (230)
daapy	577 (220)	583 (270)

[a] Not dissolved.

^{1}H NMR Spectra. NMR spectroscopy is a powerful method for studying weak interactions such as hydrogen bonding in solution. The ^{1}H NMR behavior of the NH peaks of aminopyridine derivatives was examined in order to further understand the structure of the coordination to the dirhodium core complex (Table 3).[22] The NH_2 proton peaks of ampy, apy, and dapy,

(17) Cotton, F. A.; Felthouse, T. R. *Inorg. Chem.* **1980**, *19*, 323.
(18) Ibers, J. A., Hamilton, W. C., Eds. *International Tables for X-ray Crystallography*; Kynoch: Birmingham, 1974; Vol. IV.
(19) *teXsan, Crystal Structure Analysis Package*; Molecular Structure Corporation, 1985 and 1992.
(20) (a) Cotton, F. A.; Felthouse, T. R. *Inorg. Chem.* **1981**, *20*, 600. (b) Felthouse, T. R. *Prog. Inorg. Chem.* **1982**, *29*, 73. (c) Boyar, E. B.; Robinson, S. D. *Coord. Chem. Rev.* **1983**, *50*, 109.
(21) (a) Sowa, T.; Kawamura, T.; Shida, T.; Yonezawa, T. *Inorg. Chem.* **1983**, *22*, 56. (b) Kawamura, T.; Katayama, H.; Nishikawa, H.; Yamabe, T. *J. Am. Chem. Soc.* **1989**, *111*, 8156.
(22) Chen, J.; Kostic, N. M. *Inorg. Chem.* **1988**, *27*, 2682.

Table 3. ^{1}H NMR Spectral Data of NH Protons for Axial Ligands X and $Rh_2(O_2CMe)_4$−X Systems[a]

X	metal-free X/$Rh_2(O_2CMe)_4$−X [b]
ampy	4.39/5.10 (+0.71) in $CDCl_3$
apy	4.41/5.49 (+1.08) in $CDCl_3$
dapy	4.86/5.22 (+0.36) in acetone-d_6
aampy	10.02/9.23 (−0.79) in $CDCl_3$
aapy	8.26/9.66 (+1.40) in $CDCl_3$
daapy	7.59/9.20 (+1.61) in $CDCl_3$

[a] In ppm from TMS in $CDCl_3$ or acetone-d_6. [b] The values in parentheses are the difference between the NH proton chemical shift values of metal-free ligands X and $Rh_2(O_2CMe)_4$−X systems. + and − denote a lower- and higher-field shift, respectively.

Table 4. Solid-State IR Spectral Data, ν(N−H) and ν(C═O) Stretching Vibrations, for Axial Ligands X, $Rh_2(O_2CMe)_4$, and $[Rh_2(O_2CMe)_4(X)_n]$

compound	ν(N−H)[a]	ν(C═O)[a]
$Rh_2(O_2CMe)_4$ (**1**)		1483 (ss), 1587 (ss)
ampy	3336 (wb), 3457 (wb)	
$[Rh_2(O_2CMe)_4(ampy)_2]$ (**4**)	3386 (ss), 3503 (ss)	1435 (ss), 1591 (ss)
apy	3304 (wb), 3445 (wb)	
$[Rh_2(O_2CMe)_4(apy)_2]$ (**5**)	3327 (ss), 3472 (ss)	1436 (ss), 1589 (ss)
dapy	3308 (wb), 3391 (wb)	
$[Rh_2(O_2CMe)_4(dapy)]$ (**6**)	3374 (ss), 3467 (ss)	1434 (ss), 1587 (ss)
aampy	3242 (wb)	
$[Rh_2(O_2CMe)_4(aampy)_2]$ (**7**)	3342 (ss)	1436 (ss), 1591 (ss)
aapy	3192 (wb)	
$[Rh_2(O_2CMe)_4(aapy)_2]$ (**8**)	3271 (ss)	1441 (ss), 1589 (ss)
daapy	3304 (wb)	
$[Rh_2(O_2CMe)_4(daapy)_2]$ (**9**)	3330 (ss)	1456 (ss), 1586 (ss)

[a] Frequencies in cm^{-1}. In the cases with two numerical values in one column, the former and latter values indicate asymmetric and symmetric stretching vibrations, respectively. ss and wb in the parentheses denote sharp−strong and weak−broad bands.

which were detected at 4.39, 4.41, and 4.86 ppm, respectively, exhibited a lower-field shift (5.10, 5.49, and 5.22 ppm, respectively) by the coordination to $Rh_2(O_2CCH_3)_4$. The NH proton peaks of aapy and daapy, which were observed at 8.26 and 7.59 ppm, respectively, also shifted to a lower-field region (9.66 and 9.20 ppm, respectively). The aampy complex was the only exception. Assuming that the magnitude of the lower-field shift corresponds to the strength of the hydrogen bond, the order is as follows: pyridine derivatives with two amino groups in the 2- and 6-positions > those with one amino group in the 2-position > those with amino and methyl groups in the 2- and 6-positions, although they cannot compared directly with the $Rh_2(O_2CCH_3)_4$−dapy system because of its insolubility in $CDCl_3$. The higher-field shift seen in the $Rh_2(O_2CCH_3)_4$−aampy system may be attributable to the weak hydrogen bond of the system in comparison with the stronger hydrogen bond between the aampy molecules themselves.

IR Spectra. Solid-state IR spectroscopy is very sensitive to small structural changes,[10c,23−26] and thus, it was expected to yield information about the hydrogen bonding. The properties of the hydrogen bonds between the acetato $-COO^-$ and amino $-NH/-NH_2$ groups may be reflected in their stretching vibrations. Their vibration bands for complexes **4**−**6** and **7**−**9** are listed in Table 4 together with those of complex **1** and the axial pyridine derivatives as a comparison. The symmetric and asymmetric stretching vibration bands of the μ-acetato ligand, ν_{sym}(C═O) and ν_{asym}(C═O) bands, were observed as medium and strong intensity bands at 1434−1456 and 1586−1591 cm^{-1}, respectively.[24,25] The ν_{sym}(C═O) vibration bands exhibited significantly lower-frequency shifts in comparison with $Rh_2(O_2CCH_3)_4$, although the ν_{asym}(C═O) bands were observed at almost the same frequencies as $Rh_2(O_2CCH_3)_4$. The lower-frequency shift of the ν_{sym}(C═O) band is clearly due to the hydrogen-bonding interaction. The symmetric and asymmetric stretching vibration bands of the $-NH_2$ group of complexes **4**− **6**, ν_{sym}(N−H) and ν_{asym}(N−H), were observed as strong and sharp bands at 3327−3386 and 3467−3503 cm^{-1}, respectively.[25,26] The ν(N−H) stretching vibration bands of the −NH− group for complexes **7**−**9** were also detected as strong bands at 3271−3342 cm^{-1}. It is interesting to note that all the bands were not only sharp and strong but also in the high-frequency region. This is noteworthy because the ν(N−H) vibration bands of metal-free ligands are generally detected as weak bands that shift toward the lower-frequency region by the introduction of hydrogen bonds. The higher energy shift of the ν(N−H) bands and the sharpening and increase in the intensity imply that the N−H bond was strengthened by the hydrogen bonding and can be explained as follows. The C(py)−N−H bonds attached to the pyridine ring are fixed by the hydrogen bond, which may lead to delocalization of the π-electrons through the conjugated π-orbital. This represents a unique case for the N−H stretching vibration of hydrogen bonding.

Crystal Structures of Complexes 4, 6, 7, and 9. The structures of four pyridine derivative adducts of tetrakis(μ-acetato)dirhodium(II) have been determined by single-crystal X-ray diffraction. The structural results show that the pyridine derivatives with an amino group form two kinds of dirhodium adduct linked with pyridine and amino nitrogen sites: complexes **4** and **6**. Selected bond lengths, hydrogen bond distances, and bond angles for complexes **4**, **6**, **7**, and **9** are summarized in Table 5. The structural characteristics of the four dirhodium adducts are presented below.

a. $[Rh_2(O_2CCH_3)_4(ampy)_2]$ (4). Crystal **4** contains two kinds of dirhodium adduct in the unit cell. One (**4a**) is a complex where the two axial sites of the dirhodium unit are occupied with pyridine nitrogens, and the second (**4b**) is where they are bound by the amino nitrogens. Both complexes have crystallographic inversion centers at the center of the $[Rh_2(O_2CCH_3)_4]$ core. The two crystal structures **4a** and **4b** are illustrated in parts a and b of Figure 1, respectively. The Rh−Rh separations in **4a** and **4b** are 2.417(3) and 2.400(2) Å, respectively; i.e., **4a** bound to the pyridine site showed a slightly longer Rh−Rh bond than **4b** coordinated to the amine site. A similar tendency was also seen in $[Rh_2(O_2CCH_3)_4(py)_2]$ (2.3963(2) Å)[17,20a] and $[Rh_2(O_2CC_2H_5)_4$(2,3,5,6-tetramethyl-*p*-phenylenediamine)] (2.387(1) Å)[20a] reported previously. The Rh−N(py) bond length in **4a**, 2.36(1) Å, is significantly longer than that of $[Rh_2(O_2CCH_3)_4(py)_2]$ (2.227(3) Å), although the Rh−N(amine) bond length, 2.30(1) Å, is almost the same as that of $[Rh_2(O_2CC_2H_5)_4$(2,3,5,6-tetramethyl-*p*-phenylenediamine)] (2.324(6) Å).[20a] Such an elongation in **4a** is also reported for dirhodium complexes with axial aromatic nitrogen donors having bulky rings, $[Rh_2(O_2CC_2H_5)_4$(acridine)$_2$] (2.413(3) Å)[20a] and $[Rh_2(O_2CC_2H_5)_4$(phenazine)] (2.362(4) Å);[20a] this elongation is clearly due to the steric repulsion between the 2-amino and 6-methyl groups and acetato oxygens. **4a** also exhibits apparent hydrogen bonds: N(2)···O(1) = 2.94 Å and N(2)···O(2) = 2.89 Å. The longer Rh−N bond found in **4a** may result from a competition

(23) Pneumatikakis, G.; Hadjiliadis, N. *J. Chem. Soc., Dalton Trans.* **1979**, 596.
(24) Cotton, F. A.; Feng, X. *J. Am. Chem. Soc.* **1998**, *120*, 3387.
(25) (a) Mal'kova, T. A.; Shafranskii, V. N. *Russ. J. Inorg. Chem.* **1974**, *19*, 1366. (b) Mal'kova, T. A.; Shafranskii, V. N. *J. Gen. Chem. USSR* **1975**, *45*, 618.
(26) Farrell, N.; Vargas, M. D.; Mascarenhas, Y. A.; Gambardella, M. T. do P. *Inorg. Chem.* **1987**, *26*, 1426.

Table 5. Selected Bond Lengths (Å), Hydrogen Bond Distances (Å), and Bond Angles (deg) for Complexes **4**, **6**, **7**, and **9**[a]

	4		**6**		**7**	**9**
	py coordinate	amine coordinate	py coordinate	amine coordinate	py coordinate	py coordinate
Rh−Rh′(py)	2.417(3)		2.4201(9)		2.4112(6)	2.404(1)
Rh−Rh′(am)		2.400(2)		2.398(1)		
Rh−N(py)	2.36(1)		2.365(5)		2.439(4)	2.388(6)
Rh−N(am)		2.30(1)		2.325(5)		
Rh−O(ac)	2.04(1)	2.05(1)	2.049(5)	2.047(6)	2.038(4)	2.047(4),
	2.06(1)	2.03(1)	2.030(5)	2.050(5)	2.045(3)	2.047(4)
	2.07(1)	2.05(1)	2.054(4)	2.045(5)	2.039(4)	2.052(4),
	2.04(1)	2.04(1)	2.050(5)	2.048(5)	2.028(3)	2.045(4)
N(am)···O(ac)	2.94, 2.89		3.14, 2.95		2.85, 2.94	2.89, 3.10
N(am)···O(ac)			3.02, 3.04			2.91, 2.89
Rh−Rh′−N(py)	178.0(3)		178.9(1)		178.6(1)	178.4(1)
Rh−Rh′−N(am)		176.8(4)		173.6(2)		
Rh−N(py)−C(py_4)	174.9(8)		156.9(3)		173.7(3)	162.4(3)
Rh−N(am)−C(py_2)		120(1)		120.9(4)		

[a] py, am, and ac in the parentheses denote pyridine, amine, and acetate, respectively. C(py_2) and C(py_4) are the carbon atoms at 2- and 4-positions of pyridine derivatives. The Rh and Rh′ atoms are related to a crystallographic center of inversion to each other.

of the hydrogen bonding and steric repulsion between the acetato oxygens and amino groups.

The ampy molecules coordinated to the Rh(II) atom at the amino site have Rh(2)−N(4)−C(11) and Rh(2′)−Rh(2)−N(4) angles of 120(1)° and 176.8(4)°, respectively, although coordination at the pyridine site is almost linear where the Rh(1)−N(1)−C(3) and Rh(1′)−Rh(1)−N(1) angles are 174.9(8)° and 178.0(3)°, respectively. The pyridine plane approximately bisects the acetato groups; it forms dihedral angles of 42° and 49° with the O(1)−O(3)−O(1′)−O(3′) and O(2)−O(4)−O(2′)−O(4′) planes of the bridging acetates, respectively.

b. [$Rh_2(O_2CCH_3)_4$(dapy)] (6). As is clear from the elemental analysis of complex **6**, the dapy and dirhodium molecules are contained in a 1:1 stoichiometry in the unit cell. The asymmetric unit consists of a Rh atom, two acetato ligands, and a dapy molecule. Crystallographic centers of inversion are located at the midpoint of the Rh−Rh bond and the center of the dapy molecule. The dapy molecule binds to two dirhodium units through its pyridine and amino nitrogen sites, and the two Rh atoms of the respective dirhodium unit are coordinated to the same sites of the pyridine or amino group of dapy. Complex **6**, on the whole, forms an infinite one-dimensional chain structure, as shown in Figure 2. The bond parameters around the Rh atoms are very similar to those of complex **4**. The Rh(1)−Rh(1′) bond for the py coordination site of dapy, 2.4201(9) Å, is longer than that for the amino coordination site of dapy, 2.398(1) Å. Furthermore, the Rh(1)−N(1)(py site), 2.365(5) Å, is slightly longer than the Rh(2)−N(3)(amino site), 2.325(5) Å. The coordination of dapy at the pyridine and amino sites, which is slightly different from the coordination of crystal **4**, is bent; the pyridine nitrogen coordinates to the Rh atom in a bent fashion with Rh(1)−N(1)−C(3) and Rh(1′)−Rh(1)−N(1) angles of 156.9(3)° and 178.9(1)°, respectively, and the coordination of the amino nitrogen to the Rh atom bends with Rh(2)−N(3)−C(5) and Rh(2′)−Rh(2)−N(3) angles of 120.9(4)° and 173.6(2)°, respectively. The coordination of dapy at the pyridine site is assisted by hydrogen bonds: N(2)···O(1) = 3.14 Å, N(2)···O(2) = 2.95 Å, N(3)···O(3) = 3.02 Å, and N(3)···O(4) = 3.04 Å. The pyridine plane approximately bisects the acetato groups; it forms dihedral angles of 37.6° and 51.9° with the O(1)−O(3)−O(1′)−O(3′) and O(2)−O(4)−O(2′)−O(4′) planes of the bridging acetates, respectively.

c. [$Rh_2(O_2CCH_3)_4$(aampy)$_2$] (7). The crystal structure of **7**, shown in Figure 3, consists of centrosymmetric dinuclear dirhodium cores with a Rh−Rh bond length of 2.4112(6) Å and an axially coordinated aampy with a Rh−N(1) bond length of 2.439(4) Å. The amino nitrogen of aampy, unlike in the cases of complexes **4** and **6**, does not participate in the coordination to the Rh atom. The Rh−N(1) is somewhat longer compared to those hitherto reported,[20] which evidently results from a competition of the hydrogen bond and/or steric repulsion between the acetato oxygens and amino and methyl groups: N(2)···O(1) = 2.85 Å and N(2)···O(2) = 2.94 Å. The coordination of the dapy molecule to the Rh atom is almost linear with the Rh−N(1)−C(3) and Rh′−Rh−N(1) angles of 173.7(3)° and 178.6(1)°, respectively. The pyridine plane approximately bisects the acetate groups; it forms dihedral angles of 50.3° and 41.5° with the O(1)−O(3)−O(1′)−O(3′) and O(2)−O(4)−O(2′)−O(4′) planes of the bridging acetates, respectively.

d. [$Rh_2(O_2CCH_3)_4$(daapy)$_2$] (9). The crystal structure is shown in Figure 4. The complex has a crystallographic inversion center at the center of the [$Rh_2(O_2CCH_3)_4$] core. The daapy molecules are linked to [$Rh_2(O_2CCH_3)_4$] from both apical sites with Rh−Rh and Rh−N(1) bond lengths of 2.404(1) and 2.388(6) Å, respectively, and are very similar to the three cases described above. The amino groups of daapy do not participate in coordination with the Rh atom but in hydrogen bonds with the acetato oxygens: N(2)···O(1) = 2.89 Å, N(2)···O(2) = 3.10 Å, N(3)···O(3) = 2.91 Å, and N(3)···O(4) = 2.89 Å. Although the Rh(II)−N(1) bond is clearly lengthened in comparison with [$Rh_2(O_2CCH_3)_4$(pyridine)$_2$] (2.227(5) Å),[17,20a] it is slightly shorter than the complex with acridine (2.413(3) Å)[20a] in the axial positions, [$Rh_2(O_2CCH_3)_4$(acridine)$_2$], which lengthens because of repulsion between the benzene rings of acridine and the coordinated acetato oxygens. The Rh−N bond length found here may result from a competition of the hydrogen bonding and steric repulsion between the acetato oxygens and amino groups. The coordination of daapy molecules to the Rh(II) atom results in Rh−N(1)−C(3) and Rh′−Rh−N(1) angles of 162.4(3)° and 178.4(1)°, respectively. The daapy plane approximately bisects the acetato groups; it forms dihedral angles of 49.0° and 39.6° with the O(1)−O(3)−O(1′)−O(3′) and O(2)−O(4)−O(2′)−O(4′) planes of the bridging acetates, respectively.

Thermogravimetric Measurements (TG). TG analyses between room temperature and 400 °C were performed for complexes **2**−**9**. As shown in Table 6, large characteristic mass changes were observed in the temperature range 140−290 °C. Judging from the weight percents of decreased mass, these temperatures are the result of decomposition due to a release of the axial ligands from the dirhodium adducts.[27] Interestingly,

(27) Najjar, R.; Netto, E. R.; Takano, I. *Inorg. Chim. Acta* **1984**, *89*, 53.

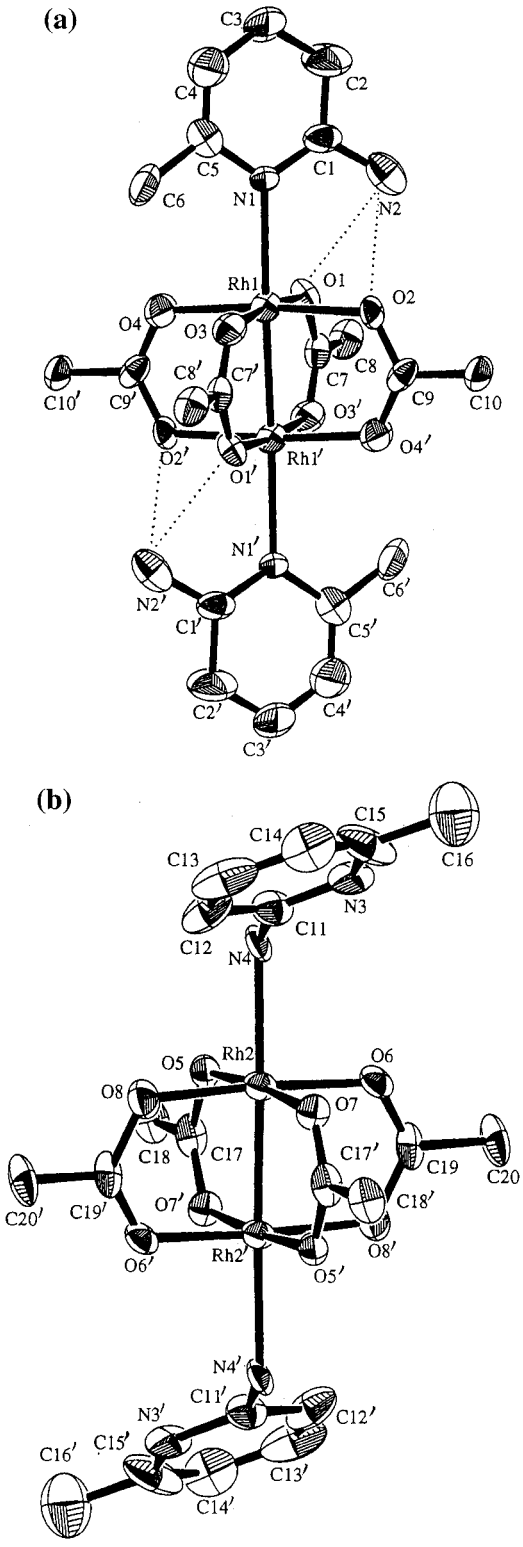

Figure 1. ORTEP drawings of **4a** (a) and **4b** (b) with label scheme. The primed and unprimed atoms are related to the crystallographic center of inversion to each other.

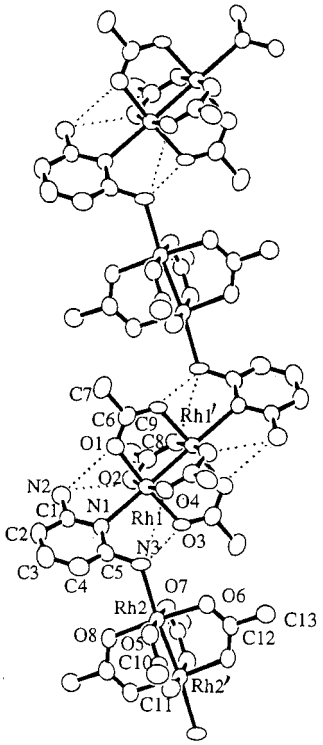

Figure 2. ORTEP drawing of complex **6** showing an infinite one-dimensional chain structure with label scheme. The primed and unprimed atoms are related to a crystallographic center of inversion to each other.

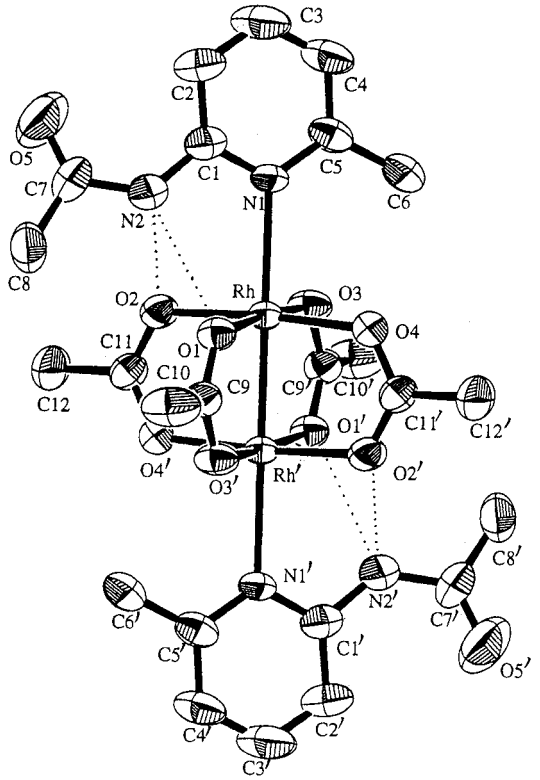

Figure 3. ORTEP drawing of complex **7** with label scheme. The primed and unprimed atoms are related to a crystallographic center of inversion to each other.

the decomposition temperatures increase in the order **4**, **7** (pyridine derivatives with 2-amino and 6-methyl groups) < **2**, **3** (those with no 2,6-substituent groups) and **5**, **8** (those with a 2-amino group) < **6**, **9** (those with 2,6-diamino groups). In the section on crystal structures, it was mentioned that the Rh−N(py) bonds in $[Rh_2(O_2CCH_3)_4(X)_n]$ (X = axial pyridine derivatives with amino and methyl groups in the 2- and 6-positions) are longer in comparison with $[Rh_2(O_2CCH_3)_4(py)_2]$ because of steric repulsions.[25b] Thus, we presumed that the decomposition temperatures of these complexes would be lower than for $[Rh_2(O_2CCH_3)_4(py)_2]$. However, Table 6 shows that the dirhodium adducts with an amino group in the 2- and/or

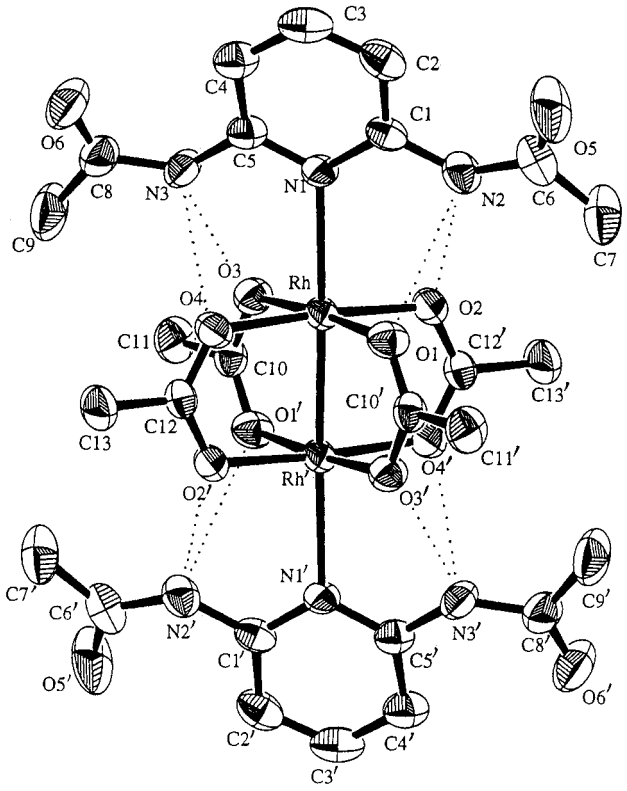

Figure 4. ORTEP drawing of complex **9** with label scheme. The primed and unprimed atoms are related to a crystallographic center of inversion to each other.

Table 6. Releasing Temperatures of Axial Ligands for $Rh_2(O_2CMe)_4$−X As Measured by TG

compound	temp[a]
$Rh_2(O_2CMe)_4(py)_2$ (**2**)	210−245
$Rh_2(O_2CMe)_4(4bupy)_2$ (**3**)	230−260
$Rh_2(O_2CMe)_4(ampy)_2$ (**4**)	145−170
$Rh_2(O_2CMe)_4(apy)_2$ (**5**)	220−240
$Rh_2(O_2CMe)_4(dapy)$ (**6**)	230−290
$Rh_2(O_2CMe)_4(aampy)_2$ (**7**)	195−225
$Rh_2(O_2CMe)_4(aapy)_2$ (**8**)	245−275
$Rh_2(O_2CMe)_4(daapy)_2$ (**9**)	250−275

[a] Temperature in °C. The two numerical values shown in the column, former and latter, indicate the temperatures at the beginning and end of releasing the axial ligands.

6-position have a higher decomposition temperature and those with a methyl group decomposed at a lower temperature. The above findings suggest that complexes **5**, **6**, **8**, and **9** are thermally stabilized by hydrogen bonds between the N−H and COO^- groups, although this is by no means an unequivocal explanation.

Conclusion

To construct a molecular assembly associated with coordinate and hydrogen bonds and to examine the effect of hydrogen bonding, eight adducts of $Rh_2(O_2CCH_3)_4$ with various axial pyridine derivatives (py, 4bupy, ampy, apy, dapy, aampy, aapy, and daapy) have been prepared. All the samples were isolated as solid precipitates, and the formulas were determined by elemental analysis. The coordination behavior of the pyridine derivatives in solution was examined by electronic absorption and ^{1}H NMR spectroscopies. The intense absorption bands assignable to the π^*(RhRh) → σ^*(RhRh) transition in $CHCl_3$ or acetone were observed at 519 nm for the dirhodium adduct with 4bupy, at 535 and 531 nm for apy and aapy, at 573 and 577 nm for dapy and daapy, and at 596 and 592 nm for ampy and aampy, respectively. The order was determined as the following: those without any substituent groups in the 2- and 6-positions > those with an amino group in the 2-position > those with two amino groups in the 2- and 6-positions > those with amino and methyl groups in the 2- and 6-positions. The formation of hydrogen bonds in dirhodium adducts has been demonstrated in $CDCl_3$ and acetone-d_6 by ^{1}H NMR spectra; the pyridine derivatives with an amino group, such as apy, aapy, ampy, aampy, dapy, and daapy, exhibited a larger downfield shift of the NH proton peaks by coordination to the Rh atom with the exception of aampy. The hydrogen bonding interaction in the solid state was studied by IR spectroscopy, X-ray diffraction, and thermogravimetric analysis. For all the dirhodium adducts with intramolecular hydrogen bonds, the ν_{sym}(C═O) stretching vibrations of the μ-acetato ligands were observed in a lower-frequency region compared with $Rh_2(O_2CCH_3)_4$ (**1**). However, the N−H stretching bands for all the pyridine derivatives with an amino group indicated interesting behavior of higher-frequency shift, sharpening, and increase of the signal intensities by the complexation. Although all the crystal structures of **4**, **6**, **7**, and **9** that were analyzed by X-ray diffraction revealed an axial coordination of the pyridine nitrogens to Rh atoms accompanied by simultaneous hydrogen bonds, the complexes **4** and **6** were also coordinated by the amino nitrogens. The effect of hydrogen bonds for the thermal stabilities of the dirhodium adducts was represented in their releasing temperatures of the axial ligands; the temperature is in the order **6**, **9** > **2**, **3**, **5**, **8** > **4**, **7** and is clearly related to the number of hydrogen bonds. Such a combination of coordinate and hydrogen bonds is useful as a building tool in designing and constructing new organic−inorganic hybridized compounds and supramolecular architectures.

Acknowledgment. This work was supported by a Grant-in-Aid for Scientific Research from the Ministry of Education, Science, Sports and Culture and partly by the Shorai Foundation for Science and Technology, to which our thanks are due.

IC991200I